

**AD-A252 368**

ARL-TR-92-7



Copy No. 41

2

**ABF Algorithms Implemented at ARL:UT**  
Technical Report under Contract N00039-91-C-0082,  
TD No. 01A1002, FDS System Engineering and Acoustics

Richard A. Gramann

**Applied Research Laboratories**  
The University of Texas at Austin  
P. O. Box 8029 Austin, TX 78713-8029

12 May 1992

Technical Report

Approved for public release; distribution is unlimited.

*Prepared for:*

**Space and Naval Warfare Systems Command**  
Department of the Navy  
Washington, D.C. 20363-5100

**S DTIC ELECTE D**  
JUL 07 1992  
**A**

**92-17626**



92

# UNCLASSIFIED

REPORT DOCUMENTATION PAGE			Form Approved OMB No. 0704-0188	
<p>Public reporting burden for this collection of information is estimated to average 1 hour per response, including the time for reviewing instructions, searching existing data sources, gathering and maintaining the data needed, and completing and reviewing the collection of information. Send comments regarding this burden estimate or any other aspect of this collection of information, including suggestions for reducing this burden, to Washington Headquarters Services, Directorate for Information Operations and Reports, 1215 Jefferson Davis Highway, Suite 1204, Arlington, VA 22202-4302, and to the Office of Management and Budget, Paperwork Reduction Project (0704-0188), Washington, DC 20503.</p>				
1. AGENCY USE ONLY (Leave blank)		2. REPORT DATE 12 May 92	3. REPORT TYPE AND DATES COVERED technical	
4. TITLE AND SUBTITLE ABF Algorithms Implemented at ARL:UT, Technical Report under Contract N00039-91-C-0082, TD No. 01A1002, FDS System Engineering and Acoustics			5. FUNDING NUMBERS N00039-91-C-0082, TD No. 01A1002	
6. AUTHOR(S) Gramann, Richard A.				
7. PERFORMING ORGANIZATION NAME(S) AND ADDRESS(ES) Applied Research Laboratories The University of Texas at Austin P.O. Box 8029 Austin, Texas 78713-8029			8. PERFORMING ORGANIZATION REPORT NUMBER ARL-TR-92-7	
9. SPONSORING/MONITORING AGENCY NAME(S) AND ADDRESS(ES) Space and Naval Warfare Systems Command Department of the Navy Washington, D.C. 20363-5100			10. SPONSORING/MONITORING AGENCY REPORT NUMBER	
11. SUPPLEMENTARY NOTES				
12a. DISTRIBUTION/AVAILABILITY STATEMENT Approved for public release; distribution is unlimited.			12b. DISTRIBUTION CODE	
13. ABSTRACT (Maximum 200 words) Two adaptive beamforming (ABF) algorithms have been implemented at ARL:UT in order to assess algorithm performance. Using data obtained with ARL:UT acoustic data acquisition systems, these algorithms are being used to assess performance of future surveillance systems. This report describes the two element-level ABF algorithms implemented thus far at ARL:UT. They are the single point constraint ABF and multiple linear constraint ABF. Both algorithms have a quadratic white noise gain constraint included in the implementation. This report also provides some details on how the algorithms have been programmed on the ARL:UT Alliant mini-supercomputer. Examples of the ABF output are also included and briefly discussed.				
14. SUBJECT TERMS adaptive beamforming (ABF) signal processing			15. NUMBER OF PAGES 27	
			16. PRICE CODE	
17. SECURITY CLASSIFICATION OF REPORT UNCLASSIFIED	18. SECURITY CLASSIFICATION OF THIS PAGE UNCLASSIFIED	19. SECURITY CLASSIFICATION OF ABSTRACT UNCLASSIFIED	20. LIMITATION OF ABSTRACT SAR	

## TABLE OF CONTENTS

	<u>Page</u>
LIST OF FIGURES.....	v
1. INTRODUCTION.....	1
1.1 BACKGROUND.....	1
2. ABF ALGORITHMS.....	3
2.1 GENERAL DESCRIPTION.....	3
2.2 SINGLE POINT CONSTRAINT ABF.....	4
2.2.1 Description and Derivation.....	4
2.2.2 Implementation on the Alliant.....	5
2.3 SINGLE POINT CONSTRAINT ABF WITH WHITE NOISE GAIN CONSTRAINT.....	6
2.3.1 Description and Derivation.....	6
2.3.2 Implementation on the Alliant.....	7
2.4 MULTIPLE LINEAR CONSTRAINTS WITH WHITE NOISE GAIN CONSTRAINT.....	10
2.4.1 Description and Derivation.....	10
2.4.2 Implementation on the Alliant.....	13
2.5 EXAMPLE BEAM PATTERNS AND SOLUTIONS.....	14
3. SUMMARY AND CONCLUSIONS.....	19
REFERENCES.....	21



Accession For	
NTIS CRA&I	M
DTIC TAB	13
Unannounced	12
Justification	
By	
Distribution/	
Availability Codes	
Dist	Availability Codes
A-1	

## LIST OF FIGURES

<u>Figure</u>		<u>Page</u>
2.1	Maximum White Noise Gain and Example Constraint (8-Element Array).....	9
2.2	Beam Pattern from SP-ABF (WNC = -100), Four Hydrophones, 60 Hz.....	15
2.3	Beam Pattern from MLC-ABF (WNC = -100), 1st Derivative=0, Four Hydrophones, 60 Hz.....	16
2.4	Beam Pattern from MLC-ABF (WNC = -100), Matched CBF at -3 dB, Four Hydrophones, 60 Hz.....	17

## **1. INTRODUCTION**

### **1.1 BACKGROUND**

Adaptive beamforming (ABF) has been in use on several of the Fleet sonar arrays for many years. It has also proven to be a useful tool to the Sound Surveillance Underwater System (SOSUS) community, enhancing sonar performance through the reduction of overall beam noise, interference rejection, and consequently enhanced detection range. Thus, ABF has become an important asset in processing line array data for passive detection problems.

It is anticipated that ABF will play a significant role in future U.S. Navy acoustic systems. Consequently, ARL:UT has implemented a variety of ABF algorithms. Several ABF algorithms have been implemented on the ARL:UT Alliant mini-supercomputer so that comparisons between these algorithms can be made on the same data, and the advantages (or disadvantages) of the different implementations explored. This document describes two of the ABF algorithms implemented, and some of the methods employed in these implementations. A previous document<sup>1</sup> describes much of the processing performed after the ABF weights have been calculated. The reader is referred to this reference for those details.

## 2. ABF ALGORITHMS

### 2.1 GENERAL DESCRIPTION

The ABF algorithms currently implemented at ARL:UT can be classified as element-level adaptive beamformers, in which the signal from each sensor is multiplied by a complex weight, and the weighted outputs summed to form the array output. The data provided to the beamformer is a cross spectral matrix (CSM) that spans a specified frequency range, for a particular set of acoustic sensors. Thus, the data have been preprocessed into the frequency domain prior to being read into the beamforming programs. The weights for each particular sensor are calculated based on this frequency domain representation of the data. Thus each sensor has one complex weight for each frequency, and the output of the array is then defined in the frequency domain as well.

The ABF algorithms described in this report can be divided into two types. The first algorithm has a single linear constraint, applied in the look direction, to assure that the array has unity gain in that direction. The second algorithm has other linear constraints in addition to the look direction constraint. The first ABF is referred to as the "single point constraint" (SP-ABF) algorithm; the second is referred to as the "multiple linear constraint" (MLC-ABF) algorithm. The types of additional linear constraints include derivative constraints and point constraints. Both are implemented in the current software. Details on each of these constraints are given Section 2.4. In addition to the linear constraint, a white noise gain constraint (WNC) has been implemented in both algorithms. The WNC is described in Sections 2.3 and 2.4.

All of the ABF algorithms discussed in this report assume plane wave signals. The arrays are assumed to be linear (i.e., straight) and sufficiently small that speed of sound variations across the array are negligible. Each sensor is assumed to be a simple omnidirectional type sensor with frequency response sufficient for the frequency ranges of interest. Further, it is assumed that the signal digitization and filtering are properly performed such that the frequency domain representations of the signals are accurate.

One final note concerning the ABF algorithms implemented at ARL:UT is necessary. We refer to these algorithms as adaptive beamforming algorithms. They are, however, the optimum beamforming solution for the type of beamformer (i.e., SP-ABF or MLC-ABF) chosen. This is referred to as an "estimate and plug" solution. The adaptive

(i.e., realtime) part of the algorithm has not been included in these implementations. In a realtime system, the weights adapt with each CSM realization, usually through a recursive algorithm. Consequently the solution depends not only on the latest CSM, but on previous CSMs and the solutions associated with them. The current implementations allow a more exact comparison between the algorithm solutions, and provide an estimate of the performance of the converged adaptive (i.e., realtime) system. Although most realtime systems use an adaptive implementation, the performance is expected to be close to that of the optimum solutions.

## 2.2 SINGLE POINT CONSTRAINT ABF

The single point constraint adaptive beamformer (SP-ABF) is described and derived below. This beamformer is not explicitly implemented on ARL:UT's Alliant computer. Rather, its solution can be obtained from the beamformer implemented with a white noise gain constraint. Hence, the Alliant implementation description is included in Section 2.3.2. However, the SP-ABF is a basic minimum variance beamformer, and its derivation shows the basic mathematical methods involved in the more complicated cases. Thus, its derivation is included here for completeness.

### 2.2.1 Description and Derivation

The SP-ABF algorithm is derived by representing the output of the array (i.e., beamformed output power) as

$$P_{ABF_{out}} = w^H R w \quad , \quad (2.1)$$

where  $w$  is the weight vector,  $H$  denotes the Hermitian (or complex conjugate) transpose, and  $R$  is the CSM. The output power of the beamformer, defined above, is minimized, subject to a single constraint. In this case, the look direction response of the array is constrained to unity gain. Restating the problem in mathematical terms gives

$$\min_w w^H R w \quad \text{subject to } w^H d = 1 \quad , \quad (2.2)$$

where  $d$  is the look direction steering vector.

To solve this problem, the method of Lagrange multipliers is used. Forming the functional that adjoins the constraint to the function to be minimized gives

$$F = w^H R w - \lambda (w^H d - 1) \quad (2.3)$$

Taking the derivative of the functional with respect to the weight vector and setting it to zero, one obtains

$$\frac{dF}{dw} = R w - \lambda d = 0 \quad (2.4)$$

Rewriting gives

$$w = \lambda R^{-1} d \quad (2.5)$$

Since  $w^H d = 1$ , one can solve for  $\lambda$ , and write the final solution for the weight vector as

$$w = \frac{R^{-1} d}{d^H R^{-1} d} \quad (2.6)$$

This is the optimum beamformer solution subject to the unity gain look direction constraint. This beamformer is often referred to as a minimum variance distortionless response (MVDR) beamformer. Unfortunately, this beamformer solution is very sensitive to sources of mismatch.<sup>2</sup> Thus a more robust beamforming solution is generally needed.<sup>3</sup> The more robust beamformer incorporates a white noise gain constraint, and is described in the next section.

### 2.2.2 Implementation on the Alliant

The MVDR (without WNC) beamformer has not been explicitly implemented on the Alliant. Rather, if a user would like this solution, the white noise gain constraint can be set to a very low value (e.g., -100 dB), essentially disabling it. Additional details are provided below.

## 2.3 SINGLE POINT CONSTRAINT ABF WITH WHITE NOISE GAIN CONSTRAINT

### 2.3.1 Description and Derivation

The SP-ABF with a white noise gain constraint is derived in a similar manner to the optimum beamformer described in the previous section. The idea behind this solution is to make the beamformer more robust, or tolerant of errors. One means of doing this is to constrain the white noise gain of the system. The white noise gain, for the MVDR beamformer, is defined as

$$G_w = \frac{1}{w^H w} \quad (2.7)$$

The white noise gain is constrained to be a value greater than or equal to the white noise gain constraint (WNC),  $\delta^2$ . By definition, the white noise gain must be less than the number of elements in the array. Thus, when constrained, the white noise gain will fall in the range

$$\delta^2 \leq G_w \leq N_{\text{elem}} \quad (2.8)$$

Thus the problem can be stated as

$$\min_w w^H R w \quad \text{subject to } w^H d = 1 \text{ and } G_w \geq \delta^2 \quad (2.9)$$

The white noise gain constraint is a quadratic inequality constraint, and thus the solution cannot be derived algebraically in closed form. The solution is the same as that of the previous optimum beamformer, except the CSM, represented by  $R$ , is replaced by a CSM that has had "white noise" injected into it. Thus, the CSM is represented by  $(R + \epsilon I)$ , where  $\epsilon$  (the second Lagrange multiplier) is increased to the extent needed to satisfy the WNC. The solution now takes the form

$$w = \frac{(R + \epsilon I)^{-1} d}{d^H (R + \epsilon I)^{-1} d} \quad (2.10)$$

Adding a small amount to the diagonal elements of the CSM (i.e.,  $\epsilon I$ ) can be thought of in several ways. It de-emphasizes the contributions of the off-diagonal elements, which decreases the relative correlation seen between those corresponding array elements. This makes the CSM appear to have weaker directional sources. Consequently the power minimization does not attempt to "null" these contributions as much as it normally would without the increased diagonal contribution. Also, by increasing the diagonal contribution, the CSM is becoming more like a CSM of only white noise (diagonal matrix). As  $\epsilon$  approaches infinity, the CSM becomes diagonally dominant, and the resulting weights are the same as those for the conventional beamformer (CBF). This is the upper limit of the white noise gain.

### 2.3.2 Implementation on the Alliant

The implementation of the SP-ABF on the Alliant involves additional derivations and equations. First, the CSM can be written in terms of its eigenvalues ( $\sigma$ ) and corresponding eigenvectors ( $U$ ). Thus

$$R = U\Sigma U^H \text{ or } U\text{diag}(\sigma)U^H \quad . \quad (2.11)$$

The CSM with white noise injected can be written similarly,

$$R + \epsilon I = U(\Sigma + \epsilon I)U^H \quad , \quad (2.12)$$

with the inverse being

$$(R + \epsilon I)^{-1} = U(\Sigma + \epsilon I)^{-1}U^H \quad . \quad (2.13)$$

The eigenvalues and eigenvectors are calculated using a singular value decomposition routine (SVD). Rewriting the weights solution in terms of the eigenvalues and eigenvectors gives

$$w = \frac{U\text{diag}\left(\frac{1}{(\sigma + \epsilon)}\right)U^H d}{d^H U\text{diag}\left(\frac{1}{(\sigma + \epsilon)}\right)U^H d} \quad . \quad (2.14)$$

Rewriting the expression for  $G_w$  in terms of the eigenvalues and eigenvectors gives

$$G_w = \frac{\left[ d^H U \text{diag} \left( \frac{1}{(\sigma + \epsilon)} \right) U^H d \right]^2}{\left[ d^H U \text{diag} \left( \frac{1}{(\sigma + \epsilon)^2} \right) U^H d \right]} \quad (2.15)$$

This equation can be broken into the part that needs to be calculated once, and the part that varies with the iteration on  $\epsilon$ . Rewriting Eq. (2.15) gives

$$G_w = \frac{\left[ \sum_k |U^H d|_k^2 \left( \frac{1}{(\sigma_k + \epsilon)} \right) \right]^2}{\left[ \sum_l |U^H d|_l^2 \left( \frac{1}{(\sigma_l + \epsilon)} \right)^2 \right]} \quad (2.16)$$

This expression (2.16) is first evaluated with  $\epsilon=0$ . If it satisfies the WNC, then no  $\epsilon$  is added to the CSM. If not, this expression is evaluated iteratively to find the proper value of  $\epsilon$  that satisfies the WNC. A version of Brent's method, adapted from *Numerical Recipes*,<sup>4,\*</sup> is used to find the value of  $\epsilon$  that satisfies the white noise constraint. Since  $\epsilon$  (as well as  $G_w$ ), can span several orders of magnitude,  $\epsilon$  is parameterized in terms of  $\log(\epsilon)$  within the searching subroutine. Once a value of  $\epsilon$  is found that satisfies the constraint, the weights are evaluated using Eq. (2.14). The weights for one look direction are calculated for all frequencies and are written to disk, prior to calculating the next look direction.

The white noise gain constraint is set relative to the maximum white noise gain possible for the array in use. In the current implementations, for frequencies above the design frequency of the array, the maximum white noise gain value is  $10 \log(N_{elem})$ , where  $N_{elem}$  is the number of sensors. This is the maximum gain attainable against spherically isotropic noise (i.e., the directivity index DI). At frequencies less than the design frequency of the array, the maximum white noise gain is set to  $10 \log(2L_a/\lambda)$ , where  $L_a$  is defined as

---

\* Function ZBRENT, pp. 253-254.

$$L_a = L \left( \frac{N_{\text{elem}}}{N_{\text{elem}} - 1} \right) = (x_{\text{max}} - x_{\text{min}}) \left( \frac{N_{\text{elem}}}{N_{\text{elem}} - 1} \right) \quad (2.17)$$

and  $x$  are the sensor locations,  $L$  is the actual distance between the end sensors (i.e.,  $x_{\text{max}}$  and  $x_{\text{min}}$ ), and  $\lambda$  is the wavelength at that frequency. These define the maximum value of white noise gain, and the WNC is set relative to these values. Figure 2.1 shows an example of the white noise gain limit and a constraint curve -3 dB relative to this maximum. The array has eight elements. Based on this constraint scheme, the white noise gain will fall on or between the two curves.

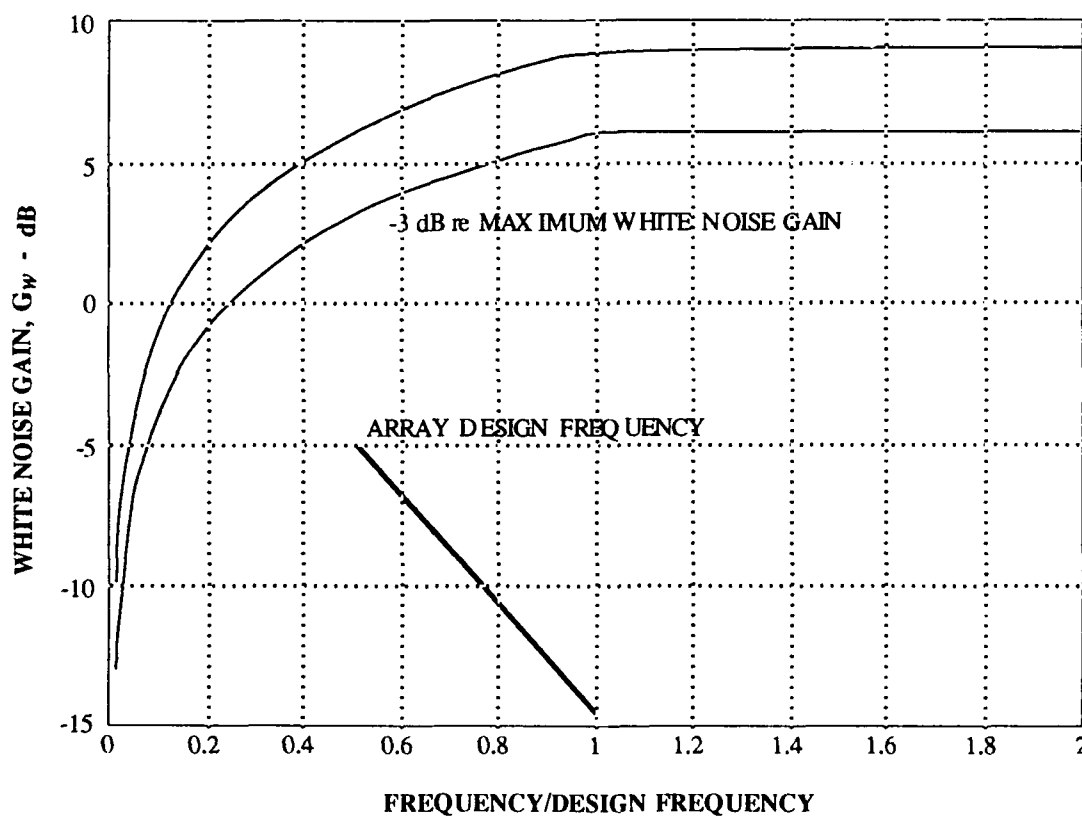


**FIGURE 2.1**  
**MAXIMUM WHITE NOISE GAIN AND**  
**EXAMPLE CONSTRAINT (8-ELEMENT ARRAY)**

**AS-92-114**

Figure 2.1 shows the current white noise gain constraint implementation. This implementation is a compromise solution that is currently being used in the existing software. Several corrections to this constraint (e.g., setting the maximum white noise gain

limit to 0 dB for very large wavelengths, accounting for variations in steering direction, etc.) will be examined in future work, and reported in a later document.

## **2.4 MULTIPLE LINEAR CONSTRAINTS WITH WHITE NOISE GAIN CONSTRAINT**

### **2.4.1 Description and Derivation**

Multiple linear constraints can be added to the beamformer solution to provide additional control of the beamformer response. These additional constraints can be used to force the beam response curve to have its first, and possibly higher derivatives equal to zero in the look direction. This type of linear constraint is known as a derivative constraint. Thus one can set the first derivative to zero in the look direction, forcing the beam response curve (i.e., the beam pattern) to be relatively flat in the vicinity of the look direction.

Another type of linear constraint is the point constraint. This constraint is used to set a specified response at locations other than the look direction. Point constraints are generally used as mainlobe maintenance constraints. One example is the "three-point constraint," where the look direction and one point on either side of the look direction is set to a specific level. Another constraint scheme might be to match the CBF beam response at specific locations on either side of the look direction. This is referred to as the Match-CBF scheme. The user selects the points (in dB) at which they wish to have the ABF beam response match the CBF beam response. This defines the location (in  $\sin \theta$  space) that these constraints are applied. They are calculated for the specific array and the locations of the constraints vary with frequency. The current implementation on the Alliant allows the user to select the response points to match the CBF pattern, and then iteratively finds the locations of those constraint points. A "three point" scheme could be to match the CBF response where the CBF response is "3 dB down." Another possible "three point" scheme could be to match the CBF response at the main response axis (MRA) of the adjacent beams in a multi-beam system. This scheme has not been implemented to date, but could easily be incorporated in the existing code. One can also specify response levels at locations relative to the look direction, which are independent of frequency. These are strictly a "user defined" point constraint.

The multiple linear constraint ABF (MLC-ABF) is derived in the same fashion as the SP-ABF. In this case, however, the look direction constraint ( $w^H d = 1$ ) is replaced with a constraint matrix and a response vector. Thus the single constraint becomes

$$M^H w = g, \quad (2.18)$$

where  $M$  is the constraint "location" matrix,  $w$  is the weights vector, and  $g$  is the response vector.

### Derivative Constraints

$M$  is constructed differently for derivative constraints than for point constraints. For derivative constraints, the first column of  $M$  is the steering vector for the look direction. Subsequent columns correspond to the derivatives of the steering vector (i.e., the second column is the 1st derivative, the third is the 2nd derivative, etc.), up to the number of derivatives being set to zero. Thus, the first column is

$$M_{k,1} = \exp\left(-j \frac{2\pi f x_k \sin(\theta)}{c}\right), \quad (2.19)$$

where  $f$  is the frequency,  $c$  is the speed of sound, and  $\theta$  is the look direction. The second column contains the 1st derivative, and is calculated using the following expression:

$$M_{k,2} = \exp\left(-j \frac{2\pi f x_k}{c}\right) M_{1,k}. \quad (2.20)$$

Higher order derivative columns then become

$$M_{k,nderiv+1} = M_{k,2} M_{k,nderiv}. \quad (2.21)$$

The response vector associated with this constraint matrix has 1 for its first element, corresponding to the look direction response, and zeroes for all of the derivative terms. Thus,  $g$  takes the form

$$g = \begin{bmatrix} 1 \\ 0 \\ 0 \\ \dots \end{bmatrix}, \quad (2.22)$$

with as many zeroes as derivatives being set.

### Point Constraints

The point constraint matrix is constructed with the columns forming the direction vectors for the constraint locations. Thus, the first column is the look direction, as before, with subsequent columns forming the look direction vectors for the additional point constraints. Hence,

$$M_{k,n} = \exp\left(-j \frac{2\pi f x_k \sin(\theta_n)}{c}\right), \quad (2.23)$$

where  $\theta_n$  are the different constraint locations. The response vector,  $g$ , contains the look direction constraint (i.e., 1) in the first element, with the other constraint responses following. For instance, if three constraints were set (i.e., look direction plus two point constraints) and these additional point constraints were set to 3 dB down,  $g$  would be

$$g = \begin{bmatrix} 1.00 \\ 0.707 \\ 0.707 \end{bmatrix}. \quad (2.24)$$

### Solution for Multiple Linear Constraints

The derivation of the solution is similar to that for the SP-ABF. Stated in mathematical terms, the problem is

$$\min_w w^H R w \quad \text{subject to } M^H w = g \text{ and } G_w \geq \delta^2. \quad (2.25)$$

Forming the functional with the multiple linear equality constraints gives

$$F = w^H R w - \lambda (M^H w - g) \quad . \quad (2.26)$$

Taking the derivative with respect to the weight vector, and solving for  $\lambda$ , gives the solution for the weight vector,

$$w = R^{-1} M [M^H R^{-1} M]^{-1} g \quad . \quad (2.27)$$

This equation shows the solution without the white noise injected. Injecting white noise replaces  $R$  with  $(R + \epsilon I)$ . Thus, the solution with the WNC included is

$$w = (R + \epsilon I)^{-1} M [M^H (R + \epsilon I)^{-1} M]^{-1} g \quad . \quad (2.28)$$

#### 2.4.2 Implementation on the Alliant

The MLC-ABF has been implemented on the Alliant for the three types of constraint schemes described above (i.e., derivative, match-CBF, and point constraints). Only one type of constraint can be used at a time with the current code. As with the SP-ABF case, the CSM is decomposed into eigenvalues and eigenvectors using an SVD subroutine (Eq. (2.11)). Based on this decomposition and the solution for the weights, the expression for the inverse of the white noise gain (i.e.,  $1/G_w$ ) can be written explicitly as

$$w^H w = \left\{ (U \text{diag}[\sigma + \epsilon]^{-1} U^H) M (M^H U \text{diag}[\sigma + \epsilon]^{-1} U^H M)^{-1} g \right\}^H \times \\ \left\{ (U \text{diag}[\sigma + \epsilon]^{-1} U^H) M (M^H U \text{diag}[\sigma + \epsilon]^{-1} U^H M)^{-1} g \right\} \quad . \quad (2.29)$$

This equation can be rewritten as

$$w^H w = \left\{ g^H [M^H U \text{diag}(\sigma + \epsilon)^{-1} U^H M]^{-1} M^H U^H \text{diag}(\sigma + \epsilon)^{-1} U \right\} \times \\ \left\{ U \text{diag}(\sigma + \epsilon)^{-1} U^H M [M^H U \text{diag}(\sigma + \epsilon)^{-1} U^H M]^{-1} g \right\} \quad . \quad (2.30)$$

This equation is broken into components that can be computed once, and those changing with iteration. Two terms computed once and stored are

$$A = U^H M \text{ and } B_{ik}^j = (M^H U)_{ij} (U^H M)_{jk} . \quad (2.31)$$

Consequently,

$$M^H U \text{diag}(\sigma + \epsilon)^{-1} U^H M \quad (2.32)$$

is computed as

$$M^H U \text{diag}(\sigma + \epsilon)^{-1} U^H M = B_{ik}^j \frac{1}{(\sigma_j + \epsilon)} . \quad (2.33)$$

Again, the iteration on white noise gain is performed if the solution without white noise injection does not satisfy the white noise gain constraint. Prior to iteration, the bounds of  $\epsilon$ , which is parameterized as  $\log(\epsilon)$ , are found using an initial bracketing routine adapted from a subroutine in *Numerical Recipes*.<sup>4,\*</sup> After the initial bounds are set, a root bracketing function using Brent's method (i.e., the same as SP-ABF) is used to find the proper  $\epsilon$  value, and the weights are calculated and stored for that frequency. After completing all frequencies in the CSM, the weights for that look direction are written to disk.

## 2.5 EXAMPLE BEAM PATTERNS AND SOLUTIONS

Figures 2.2 through 2.4 show examples of beam patterns calculated from the ABF weights for the different algorithms described above. All were calculated using the same four CSMs and the same array configurations. The CSMs were calculated from timeseries data obtained from a horizontal line array in a deep ocean environment. The time period between each CSM is approximately 15 s. In all cases, the white noise gain constraint was turned off (WNC = -100 dB). The range of  $\sin \theta$  in each figure is -2 to 2, thus showing the beam pattern in visible and invisible space. This allows inspection of the sidelobe structure. Also, mainlobe squinting at look directions near endfire can be seen more easily with this format.

---

\* Subroutine ZBRAC, pp. 245-246.

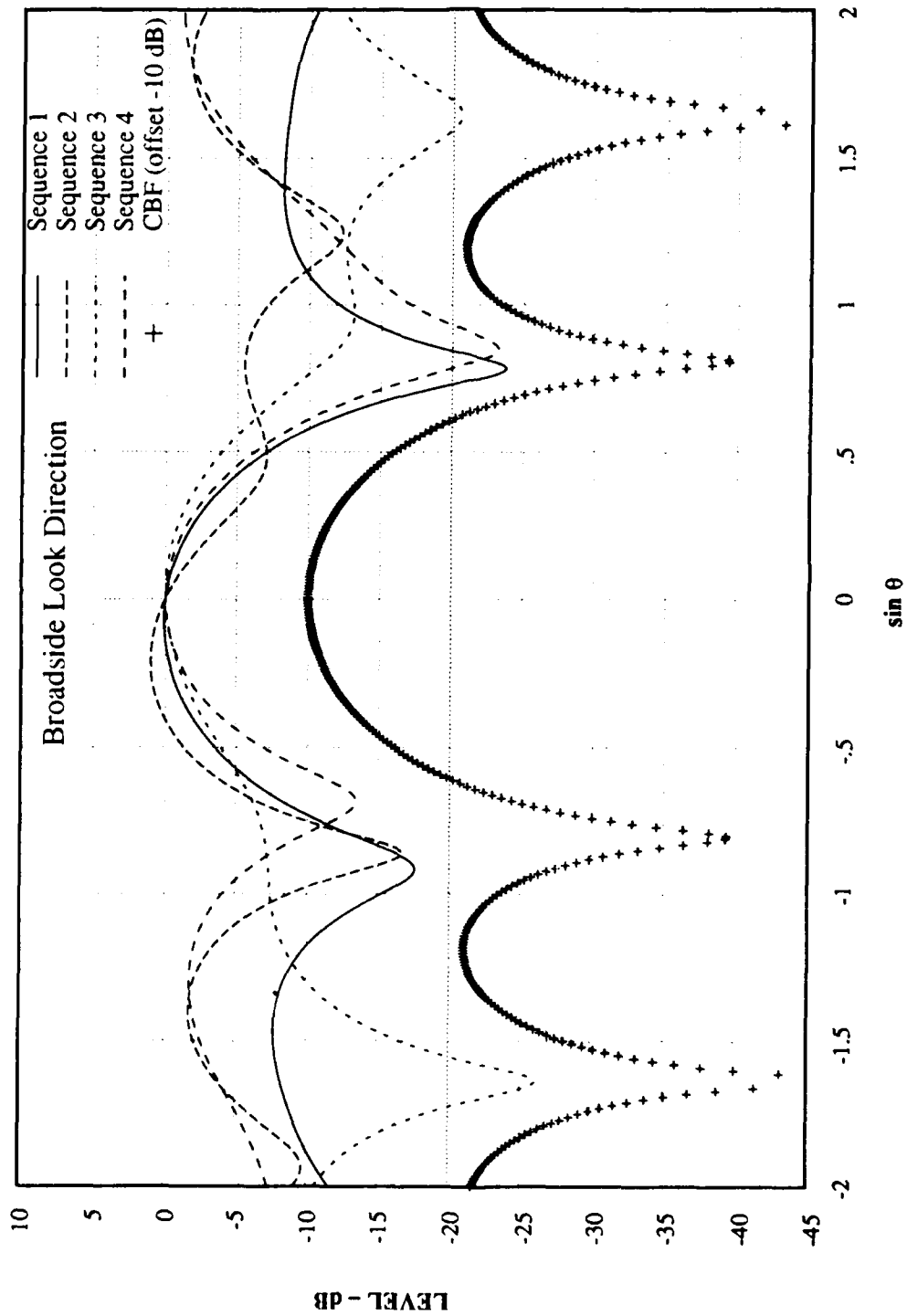


**FIGURE 2.2**  
**BEAM PATTERN FROM SP-ABF (WNC = -100),**  
**FOUR HYDROPHONES, 60 Hz**

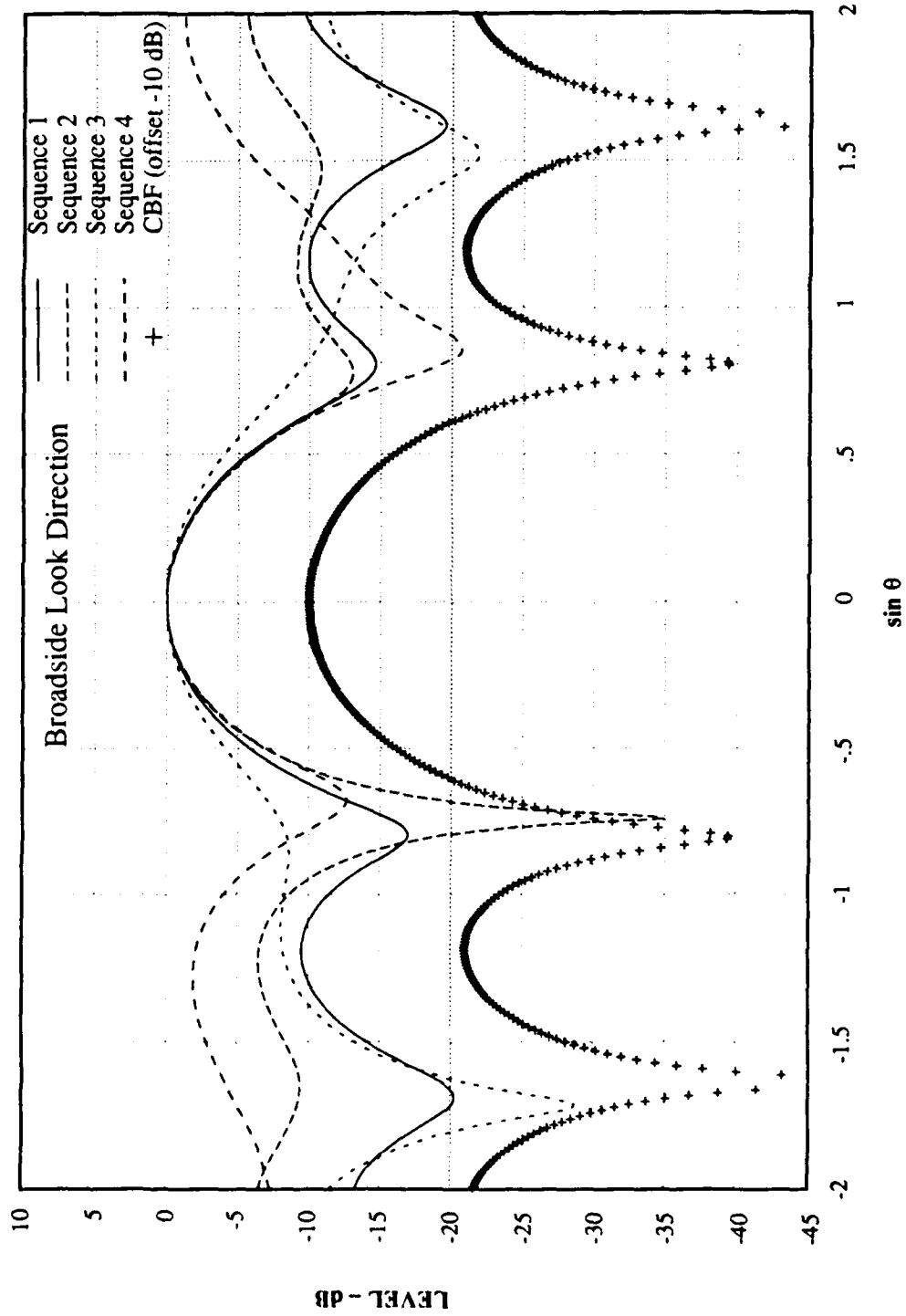


**FIGURE 2.3**  
**BEAM PATTERN FROM MLC-ABF (WNC = -100), 1st DERIVATIVE = 0,**  
**FOUR HYDROPHONES, 60 Hz**

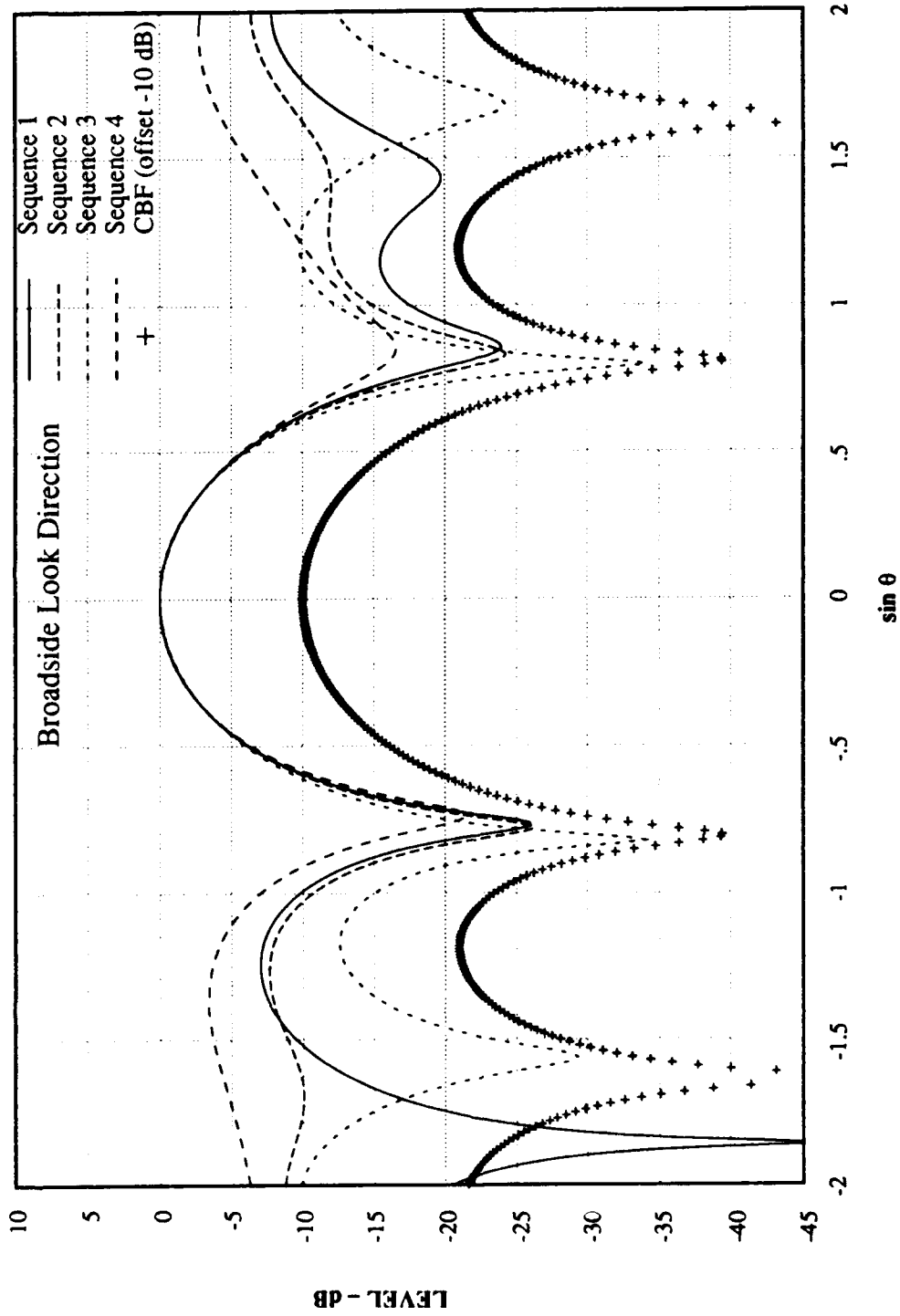


**FIGURE 2.4**  
**BEAM PATTERN FROM MLC-ABF (WNC = -100), MATCHED CBF AT -3 dB,**  
**FOUR HYDROPHONES, 60 Hz**

Figure 2.2 shows the beam patterns based on the SP-ABF, and the equivalent CBF beam pattern. The CBF beam pattern is offset -10 dB for clarity. Clearly, each of the beam patterns satisfies the look direction constraint of unity gain (0 dB response). However, the slope of the response curves in the look direction, as well as the shapes of the mainlobes vary with the different input CSMs.

Figure 2.3 shows the beam pattern calculated from weights generated with the MLC-ABF program, with the first derivative set to zero in the look direction. The slope of each curve is zero at the look direction, and the response is much flatter (and closer to 0 dB) at locations near the look direction than in Figure 2.2.

Finally, Figure 2.4 shows the beam pattern calculated with weights generated with the MLC-ABF program using the Match-CBF option. In this case, a "three point" constraint was set with the two mainlobe maintenance constraints set to match the CBF response at the "3 dB down" points. Now, all of the response curves have essentially the same mainlobe shape between  $\sin \theta = -0.4$  and  $0.4$ .

### 3. SUMMARY AND CONCLUSIONS

Two adaptive beamforming (ABF) algorithms have been implemented at ARL:UT in order to assess the achievable performance of ABF. The single point (look direction) constrained (SP-ABF) and multiple linear constrained (MLC-ABF) adaptive beamformers were derived and explanations of their implementation were given in the previous sections. A discussion of the white noise gain constraint and its implementation was also included. Additional work examining the performance of these algorithms is under way using data obtained with ARL:UT acoustic data acquisition systems, and will be reported in a later document.

## REFERENCES

1. F. W. Machell, "Algorithms for Broadband Processing and Display," Applied Research Laboratories Technical Letter No. 90-8 (ARL-TL-EV-90-8), Applied Research Laboratories, The University of Texas at Austin, March 1990.
2. H. Cox, "Resolving Power and Sensitivity to Mismatch of Optimum Array Processors," *J. Acoust. Soc. Am.* 54(3), 771-785 (1973).
3. H. Cox, R. M. Zeskind, and M. M. Owen, "Robust Adaptive Beamforming," *IEEE Trans. Acoustics, Speech, and Signal Processing* ASSP-35 (10), 1365-1376 (1987).
4. W. H. Press, B. P. Flannery, S. A. Teukolsky, and W. T. Vetterling, *Numerical Recipes* (Cambridge University Press, New York, 1986).

12 May 1992

**DISTRIBUTION LIST FOR  
ARL-TR-92-7  
Technical Report under  
Contract N00039-91-C-0082, TD No. 01A1002,  
FDS System Engineering and Acoustics**

Copy No.

1 Commander  
2 Space and Naval Warfare Systems Command  
3 Department of the Navy  
4 Washington, D.C. 20363-5100  
5 Attn: CAPT K. Evans (PD80)  
6 C. Andriani (PD80T)  
7 L. Parish (PMW181T)  
8 J. P. Feuillet (PMW182-21)  
9 L. Fabian (PMW183-4)  
R. Hobart (PMW184)  
CAPT (sel) W. Hatcher (PMW184T)  
CDR R. Goldsby (PMW184A)  
CDR J. Liechty (PMW184-3)

10 - 11 Office of the Assistant Secretary of the Navy  
(Research, Development, and Acquisition)  
Department of the Navy  
Washington, D.C. 20350-1000  
Attn: G. Cann

12 Office of the Deputy Assistant Secretary of the Navy  
13 Antisubmarine Warfare Programs  
Department of the Navy  
Washington, D.C. 20350-1000  
Attn: A. Bisson  
CDR D. Backes

14 Office of the Chief of Naval Operations  
15 Department of the Navy  
Washington, D.C. 20350-2000  
Attn: J. Schuster (OP-02T)  
CAPT F. Crawford (OP-24)

16 Office of the Chief of Naval Operations  
Naval Observatory  
34th and Massachusetts Ave.  
Washington, D.C. 20390  
Attn: R. Winokur (Code 096T)

Distribution List for ARL-TR-92-7  
Under Contract N00039-91-C-0082, TD No. 01A1002  
(cont'd)

Copy No.

17	Office of the Chief of Naval Research Department of the Navy Arlington, VA 22217-5000 Attn: R. Feden (Code 124A)
18	Office of the Chief of Naval Research Office of Naval Technology Department of the Navy Arlington, VA 22217-5000 Attn: A. Faulstich (ONT23) CAPT R. Fitch (ONT23D) T. Goldsberry (ONT231)
19	
20	
21	Defense Advanced Research Projects Agency 1400 Wilson Blvd. Arlington, VA 22209 Attn: C. Stuart
22	Commander Naval Air Systems Command Department of the Navy Washington, D.C. 20361-7121 Attn: E. Benson (PMA264)
23	Commander Naval Research Laboratory Washington, D.C. 20375-5000 Attn: D. Bradley (Code 5100) W. Smith (Code 5150)
24	
25	Commanding Officer Naval Command Control and Ocean Surveillance Center RDT&E Division San Diego, CA 92152-5000 Attn: D. Hanna (Code 705) R. Harris (Code 723) D. Barbour (Code 733)
26	
27	
28	Commanding Officer Naval Air Development Center Warminster, PA 18974 Attn: L. Allen
29	Superintendent Naval Postgraduate School Monterey, CA 93940 Attn: Library

Distribution List for ARL-TR-92-7  
Under Contract N00039-91-C-0082, TD No. 01A1002  
(cont'd)

Copy No.

30-41 Commanding Officer and Director  
Defense Technical Information Center  
Cameron Station, Building 5  
5010 Duke Street  
Alexandria, VA 22314  
Attn: Library

42 Director  
North Atlantic Treaty Organization  
SACLANT ASW Research Centre  
APO New York 09019  
Attn: Library

43 Applied Physics Laboratory  
The Johns Hopkins University  
Johns Hopkins Road  
Laurel, MD 20810  
Attn: J. Lombardo  
44 A. Boyles  
45 K. McCann  
46 R. Mitnick  
47 B. Newhall

48 Bolt, Beranek, and Newman  
1300 North 17th Street  
Arlington, VA 22209  
Attn: M. Flicker

49 Bell Telephone Laboratories, Inc.  
P.O. Box 496  
Whippany, NJ 07981-0903  
Attn: J. Eickmeyer  
50 R. Patton

51 The Mitre Corporation  
7525 Colshire Drive  
McLean, VA 22102  
Attn: K. Hawker

52 ORINCON  
1755 Jefferson Davis Highway  
Arlington, VA 22202  
Attn: H. Cox

53 Planning Systems, Inc.  
7900 Westpark Drive, Suite 507  
McLean, VA 22101  
Attn: D. Pickett

Distribution List for ARL-TR-92-7  
Under Contract N00039-91-C-0082, TD No. 01A1002  
(cont'd)

Copy No.

54	Science Applications International Corporation 1710 Goodridge Drive McLean, VA 22101 Attn: J. Hanna
55	TRW, Inc. TRW Defense & Space Systems Group Washington Operations 7600 Colshire Drive McLean, VA 22101 Attn: R. Brown
56	B. O'Rear
57	L. Thorne
58	Department of Physics The University of Auckland Private Bag, Auckland NEW ZEALAND Attn: A. C. Kibblewhite
59	C. T. Tindle
60	Environmental Sciences Group, ARL:UT
61	Hans A. Baade, ARL:UT
62	Nancy R. Bedford, ARL:UT
63	Glen E. Ellis, ARL:UT
64	Karl C. Focke, ARL:UT
65	Richard A. Gramann, ARL:UT
66	David E. Grant, ARL:UT
67	Robert A. Koch, ARL:UT
68	Fredrick W. Machell, ARL:UT
69	Stephen K. Mitchell, ARL:UT
70	Clark S. Penrod, ARL:UT
71	Carol V. Sheppard, ARL:UT
72	Jack A. Shooter, ARL:UT
73	Evan K. Westwood, ARL:UT

Distribution List for ARL-TR-92-7  
Under Contract N00039-91-C-0082, TD No. 01A1002  
(cont'd)

<u>Copy No.</u>	
74	Bruce G. Williams, ARL:UT
75	Gary R. Wilson, ARL:UT
76	Library, ARL:UT
77	Reserve, ARL:UT